# Morphology of Vergina Star 16-Arm Block Copolymers and Scaling Behavior of Interfacial Area with Graft Point Functionality

**ARTICLE** *in* MACROMOLECULES · APRIL 1997

Impact Factor: 5.8 · DOI: 10.1021/ma961855s



**5 AUTHORS**, INCLUDING:

Apostolos Avgeropoulos
University of Ioannina
**123** PUBLICATIONS **1,794** CITATIONS
SEE PROFILE

Hadjichristidis Nikos
King Abdullah University of Science and Tech…
**301** PUBLICATIONS **8,973** CITATIONS
SEE PROFILE

# Morphology of Vergina Star 16-Arm Block Copolymers and Scaling Behavior of Interfacial Area with Graft Point Functionality

**Frederick L. Beyer and Samuel P. Gido***

*W. M. Keck Electron Microscopy Laboratory, Polymer Science and Engineering Department, University of Massachusetts, Amherst, Massachusetts 01003*

**Yiannis Poulos, Apostolos Avgeropoulos, and Nikos Hadjichristidis†**

*Department of Chemistry, University of Athens, Panepistimiopolis Zografou 15771, Athens, Greece*

*Received December 17, 1996; Revised Manuscript Received February 7, 1997*[⊗]

ABSTRACT: The morphological behavior of three well-defined miktoarm star block copolymers having 16 arms/molecule was characterized using transmission electron microscopy (TEM), small-angle X-ray scattering (SAXS), and small-angle neutron scattering (SANS) techniques. The molecules, called *Vergina* stars, have 8 arms of polyisoprene and 8 arms of polystyrene radiating from a single junction point. The samples, with polystyrene volume fractions of 0.37, 0.44, and 0.47 and total molecular weights ranging from 330 000 to 894 000, were all found to microphase separate into lamellar morphologies. In this respect all three samples, in agreement with theory, behave in the same way as linear diblock copolymers of the same relative volume fractions. Incorporating results from previous studies in the literature of miktoarm block copolymers containing trifunctional and tetrafunctional branch points, as well as the new Vergina star data, the scaling behavior of the area per junction versus junction functionality was investigated.

## Introduction

Star block copolymers are a class of nonlinear block copolymers which, like other block copolymers, microphase separate due to incompatibility between the two polymer materials comprising the distinct blocks. We have been pursuing the effect of controlled chain grafting architecture on microphase-separated morphology through several series of architecturally controlled materials.[1−3] As illustrated in Figure 1, the Vergina stars have a total of 16 arms, 8 arms of polystyrene (PS) and 8 arms of polyisoprene (PI), which are joined together at a single junction. As the figure implies, the junction chemistry is such that the PS and PI arms both radiate in all directions. In the microphase-separated state, however, the arms a short distance from the junction point have segregated by material type. In the notation of Olvera de la Cruz and Sanchez, the Vergina star block copolymers are of the type $A_nB_n$, with A = PS, B = PI, and $n = 8$.[4] Hadjichristidis has termed this general type of architecture, which has multiple *arms* radiating from a central junction point, *miktoarm* stars meaning *mixed arm*. The name *Vergina* comes from the town in northern Greece near which the ancient tomb of King Phillipos of Macedonia was discovered by the late Prof. M. Andronikos, of the University of Thessaloniki. Inside the tomb was a golden larnax (chest) with the depiction of a 16-rayed star, from which the Vergina star architecture was conceived.

The multiarm, Vergina star copolymers investigated in this paper form morphologies in which the relationship between domain dimensions and molecular weight is significantly altered from what is commonly observed in linear block copolymers. Due to the highly branched structure of the Vergina star molecules, the spacing of junction points along the interface is significantly larger than that for any previously studied linear or miktoarm diblock copolymer.

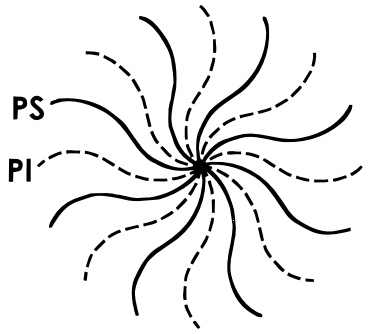


**Figure 1.** Vergina star; the 16-armed miktoarm star block copolymer architecture with 8 PS arms and 8 PI arms.

Based on the weak segregation theory predictions of Olvera de la Cruz and Sanchez, it was expected that the Vergina stars would microphase separate into the same morphologies as those observed in linear diblocks of the same relative volume fractions, due to the overall symmetry of the Vergina molecules.[4] This prediction is also consistent with the strong segregation theory for microphase-separated miktoarm star copolymers formulated by Milner.[5] Milner's theory predicts shifting of the observed morphologies from those observed for a simple linear diblock as a result of asymmetry in the number of arms of components A and B and of asymmetry in the chain characteristics (stiffness and volume per segment) of the A and B materials. Milner's model uses the $\epsilon$ parameter, defined by $\epsilon = (n_A/n_B)(l_A/l_B)^{1/2}$, where $n_i$ is the number of graft arms of block type $i$ (A or B) and $l_i = V_i/R_{gi}^2$. Here $V_i$ is the volume of an entire arm of material $i$, and $R_{gi}^2$ is the mean-square radius of gyration of an arm of material $i$. The parameter $l_i$ gives a measure of the space-filling characteristics of the polymer chain. In the case of the symmetrical Vergina stars, $\epsilon$ reduces to $(l_{PS}/l_{PI})^{1/2}$. For blocks of PI and PS, one calculates a value for $\epsilon$ that is close to unity (1.16). Therefore, the predicted morphologies are essentially the same as those of PS−PI linear diblocks.

A total of three samples was prepared for the present study; detailed molecular characterization of these

* To whom correspondence should be addressed.
† Also at FORTH-IESL, 711 10 Heraklion, Crete, Greece.
[⊗] Abstract published in *Advance ACS Abstracts,* April 1, 1997.

S0024-9297(96)01855-4 CCC: $14.00 

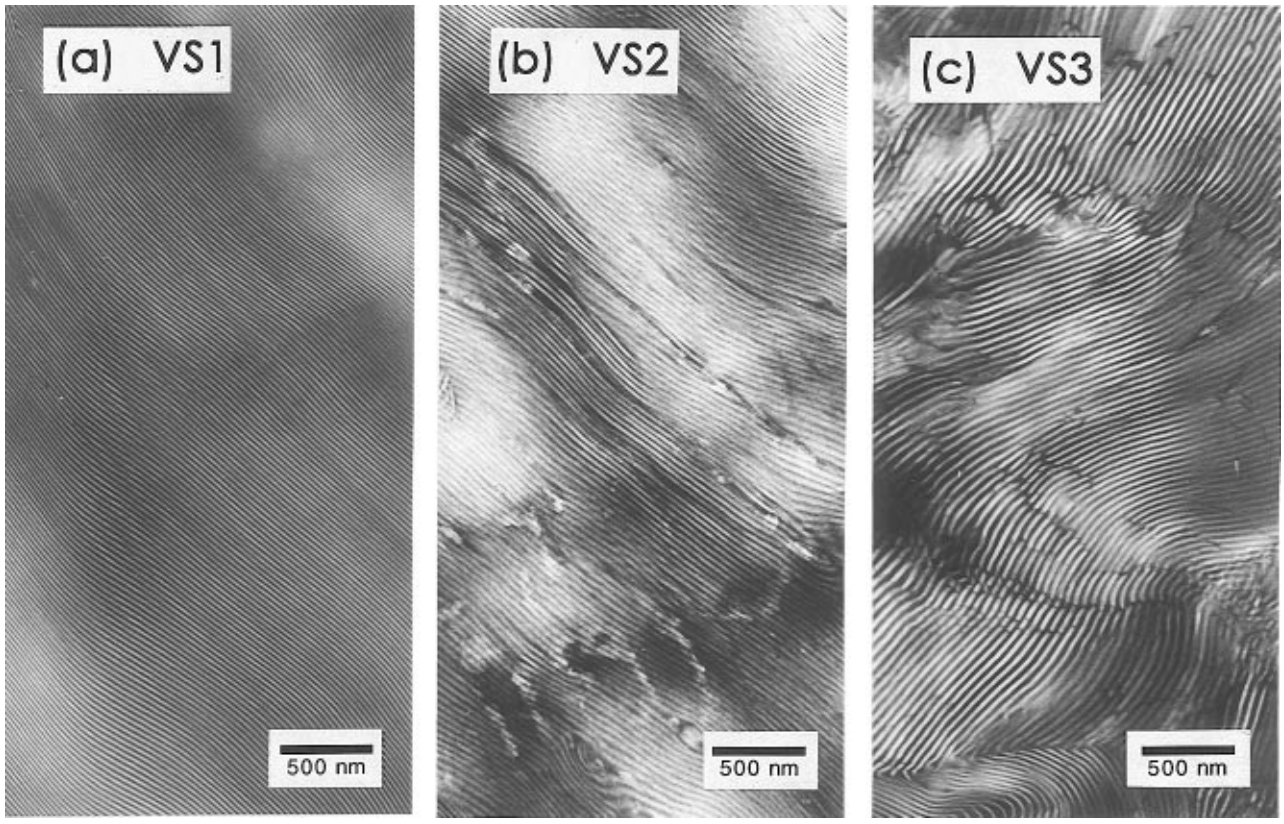


**Figure 2.** TEM images of the lamellar morphologies of samples VS1 (a), VS2 (b), and VS3 (c).

materials is given in ref 6. Two of these Vergina star materials had nearly the same relative volume fractions of PS and PI, but different overall molecular weights of 330,000 g/mol and 710,000 g/mol. The lower molecular weight sample, VS1, had a PS volume fraction of 0.44, and the larger molecular weight sample, VS2, had a PS volume fraction of 0.47. These two samples were expected to exhibit lamellar morphologies. The third sample, VS3, had a PS volume fraction of 0.37 and a molecular weight of 894,000 g/mol. It is also expected to be lamellar, although it falls near the boundary where a transition to a cubic bicontinuous or cylindrical structure would be expected.

## Experimental Section

Synthesis of the Vergina star block copolymers has been described in a previous publication.[6] The PS and PI arms are synthesized separately using high-vacuum, anionic polymerization techniques. These arms are then linked together using chlorosilane coupling chemistry to form the final Vergina star molecule.

Solid films approximately 1 mm thick of the Vergina star polymers were cast from a 2 wt % toluene solution in 30 mL Pyrex beakers. Toluene is a nearly nonselective solvent for PS and PI. The rate at which the solvent evaporated was regulated so that the polymer films formed slowly over a 2-week period. The films were kept at room temperature and atmospheric pressure for several more days to allow continued evaporation of solvent. The samples were then placed under high vacuum at room temperature to allow further evaporation of residual solvent. They were then annealed for 1 week at 115 °C, following a 2-day period in which the oven temperature was slowly increased from room temperature. The samples were then allowed to cool slowly to room temperature over a period of 2 days.

All samples studied by transmission electron microscopy (TEM) were microtomed using a Leica cryoultramicrotome. Sections approximately 500 Å thick were cut from bulk films of sample mounted in epoxy using a Diatome cryo diamond knife. During sectioning, the samples were held at −110 °C while the knife was kept at −95 °C. Sections were collected on TEM grids and then stained for 4 h in $OsO_4$, which reacts with the double bonds of the PI blocks and renders the PI domains dark relative to the PS domains in mass-thickness contrast imaging. TEM imaging was performed using a JEOL 100CX electron microscope operated at an accelerating voltage of 100 kV.

Small-angle X-ray scattering (SAXS) experiments were performed on both annealed and unannealed specimens using a Rigaku-Denki camera with Cu Kα sealed-tube X-ray radiation and pinhole collimation. Patterns were recorded photographically with Kodak direct-exposure X-ray film (DEF5). SAXS patterns were digitized with an Agfa Arcus II flat-bed scanner and analyzed with custom-written software. Small-angle neutron scattering (SANS) was performed at the Cold Neutron Research Facility at the National Institute of Standards and Technology, Gaithersburg, MD. Although our samples were not deuterated, their well-ordered structures produced sufficient neutron scattering for structural analysis. Samples were placed in the beam of the NG3-SANS, with the incident radiation parallel to the surface of the cast films. Camera lengths of 3 and 13 m were used at a wavelength of 5 Å. The NG3 uses pinhole collimation of the monochromated beam.

## Results

All three Vergina stars formed lamellar morphologies, as is shown in Figure 2. Figure 3 shows representative SANS data from each sample, recorded at the longer camera length of 13 m. Table 1 gives molecular characteristics and lamellar long periods determined by SANS.

Figure 2a shows a TEM image of the lamellar microstructure of VS1, in which extremely well-ordered microdomains are evident. Large coherently ordered regions of lamellar structure were commonly seen in all TEM experiments on VS1. The SANS data for VS1 in Figure 3 show 2 orders of reflection from the lamellar long period, $L$, of 371 ± 6 Å. VS2 was similar to VS1 in many respects, including the nearly equal volume fractions of both constituent blocks. Figure 2b shows a typical example of the VS2 lamellar morphology ob-

**Table 1. Molecular Characteristics and Scaling Behavior of Lamella Forming Miktoarm Star Block and Diblock Copolymers**

| sample (reference) | $M_n$ | PDI | $\phi_{PS}$ | $M_n$/PS arm | PS arms/junction | $M_n$/PI arm | PI arms/junction | $L$ (nm) | $A/R_g^2$ | $AN^{2/3}/R_g^2$ |
|---|---|---|---|---|---|---|---|---|---|---|
| L1 (7) | 21 000 | 1.16 | 0.50 | 11 000 | 1 | 10 000 | 1 | 17 | 0.211 | 8.43 |
| L2 (7) | 31 000 | 1.13 | 0.37 | 12 000 | 1 | 19 000 | 1 | 24 | 0.145 | 7.75 |
| L3 (7) | 49 000 | 1.13 | 0.42 | 22 000 | 1 | 27 000 | 1 | 28 | 0.112 | 8.01 |
| L4 (7) | 55 000 | 1.18 | 0.43 | 25 000 | 1 | 30 000 | 1 | 34 | 0.105 | 8.11 |
| L5 (7) | 97 000 | 1.18 | 0.48 | 45 000 | 1 | 52 000 | 1 | 46 | 0.077 | 8.66 |
| L6 (7) | 102 000 | 1.18 | 0.58 | 62 000 | 1 | 40 000 | 1 | 51 | 0.074 | 8.26 |
| S2I-49 (8) | 75 400 | 1.06 | 0.51 | 20 800 | 2 | 33 800 | 1 | 36.1 | 0.121 | 11.3 |
| I3S-55 (8) | 101 900 | 1.05 | 0.55 | 59 300 | 1 | 14 200 | 3 | 39.2 | 0.133 | 15.0 |
| I3S-61 (8) | 94 400 | 1.05 | 0.61 | 59 300 | 1 | 11 700 | 3 | 38.0 | 0.134 | 14.1 |
| I2S-3 (2) | 83 000 | 1.04 | 0.62 | 61 200 | 1 | 14 800 | 2 | 39.0 | 0.113 | 11.5 |
| VS1 (6) | 330 000 ($M_w$) | 1.07 | 0.44 | 20 900 ($M_w$) | 7.7 | 20 200 ($M_w$) | 8.4 | 37.1 | 0.362 | 91.9 |
| VS2 (6) | 710 000 ($M_w$) | 1.05 | 0.47 | 43 600 ($M_w$) | 7.9 | 48 200 ($M_w$) | 7.6 | 51.5 | 0.244 | 103 |
| VS3(6) | 894 000 ($M_w$) | 1.05 | 0.37 | 43 600 ($M_w$) | 7.9 | 71 200 ($M_w$) | 7.7 | 64.1 | 0.174 | 87.8 |

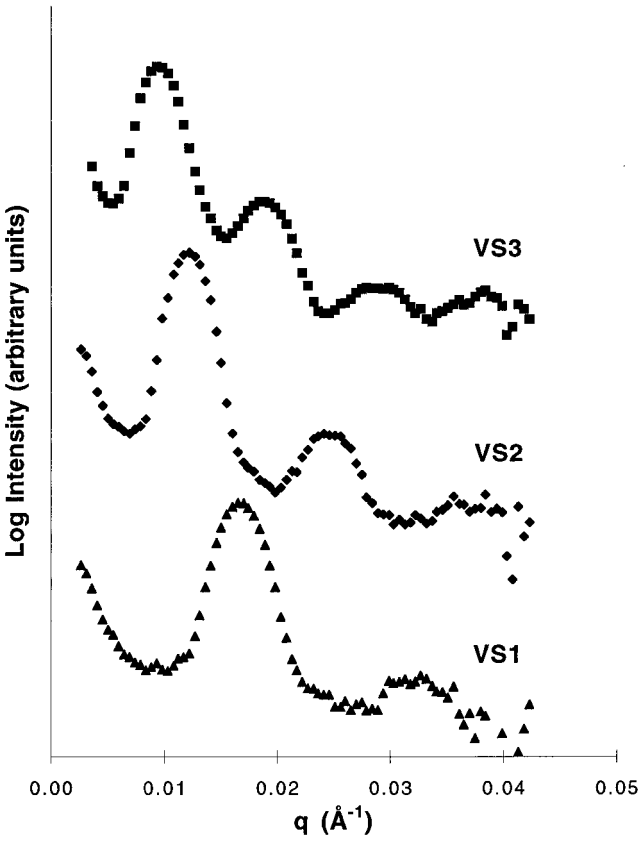


**Figure 3.** SANS intensity vs scattering vector, $q$, for VS1, VS2, and VS3.

served in TEM. SAXS and SANS both provided conclusive evidence of the lamellar morphology with $L = 515 \pm 6$ Å. Three orders of reflection are visible in the SANS pattern shown in Figure 3. VS3, with significantly more asymmetric volume fractions, also exhibited a lamellar morphology. Figure 2c shows a TEM image of the VS3 lamellar morphology. SANS results, shown also in Figure 3, clearly demonstrate the lamellar character of the microphase-separated domains, displaying 4 orders of reflection from $L = 641 \pm 6$ Å.

## Discussion

The three Vergina star samples characterized in this paper, when combined with data from previous studies of linear diblocks and less highly branched miktoarm star architectures, permit the examination of the effect of graft point functionality on microphase-separated domain dimensions. Table 1 lists molecular characteristics and microphase-separated lamellar long spacings for a number of PS−PI diblocks, $I_2S$ and $S_2I$ tribranched architectures, $I_3S$ tetrabranched architectures, as well as the Vergina stars. The data on the other materials are obtained from our previous work and from the literature.[2,7,8] Of particular interest is how the graft point functionality effects the interfacial area per molecule. From previous results on diblock copolymers, we are accustomed to block copolymers stretching normal to the interface between microphase-separated domains so that $L \sim N^{2/3}$ is obtained in strongly segregated systems. Through conservation of volume in these incompressible materials, the molecular dimensions in the plane of the interface, and thus the area per molecule, $A$, must be correspondingly reduced such that $A \sim N^{1/3}$.

We now examine the behavior of the dimensionless area per molecule as a function of junction functionality. The dimensionless area per molecule is defined as $A/R_g^2$, the ratio of the area to the mean-square radius of gyration of the entire star-shaped molecule. The area per molecule is simply the volume of a molecule divided by half the long spacing, where the volume of the molecule is estimated based on known density values for bulk PS and PI. Values of this parameter are given for all the materials in Table 1. For diblocks we calculate $R_g$ according to the standard relationship for linear chains using a number-weighted average Kuhn length. For 3- and 4-armed miktoarm star block copolymers $R_g$ is determined using the Zimm−Stockmeyer approach for the calculation of $g = R_g/R_L$, where $R_L$ is the radius of gyration of a linear polymer chain with the same total number of repeat units as the entire star molecule.[9] This approach, which is based on Gaussian statistics, does not properly account for the high degree of crowding and the resultant chain stretching near the junction point of a star molecule with a large number of arms like the Vergina stars. Thus, this standard calculation underestimates $R_g$ for many-armed stars. Published comparisons of experimentally determined and calculated $R_g$ values for 12- and 18-arm stars[10] allow us to estimate, by interpolation, that calculated $g$, and thus $R_g$, values for the Vergina stars must be increased by a factor of 1.45 to account for expansion due to arm crowding. The resulting $R_g$ values for the Vergina stars are consistent with experimental determinations of $R_g$ for the same series of Vergina stars.[11] Also, the $g$ values we obtained are consistent with an extrapolation of the experimental data in Table III of Daoud and Cotten's paper[12] to 16-arm stars utilizing the Θ condition scaling relationship in their eq 25. The dimensionless area per molecule still has a molecular weight (degree of polymerization) dependence which, in the strong segregation limit, scales as $N^{-2/3}$. Thus, we define the molecular weight corrected, dimen-

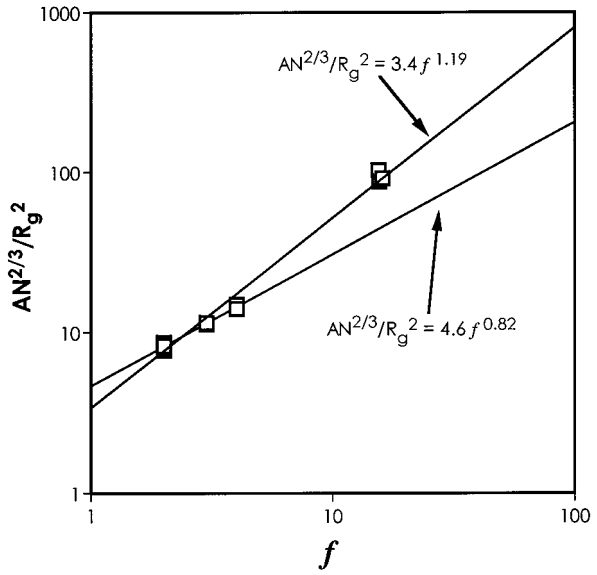


**Figure 4.** log−log plot of $AN^{2/3}/R_g^2$ vs graft point functionality, $f$, for diblocks, 3- and 4-armed miktoarm stars and the Vergina stars.

sionless area per molecule as $AN^{2/3}/R_g^2$. This parameter is also given for each material in Table 1.

Figure 4 shows a log−log plot of $AN^{2/3}/R_g^2$ vs graft point functionality, $f$ = total number of arms. A least-squares fit yields the power law expression $AN^{2/3}/R_g^2 = 3.4f^{1.19}$. Excluding the Vergina star data, the points for diblock, 3- and 4-armed stars can be better fit to the expression $AN^{2/3}/R_g^2 = 4.6f^{0.82}$. This discrepancy may be caused by an underestimation of $R_g$ for the Vergina stars even after we have applied an expansion factor of 1.45. It could also result from the fact that the diblock, 3- and 4-armed stars all have only 1 arm of at least one of the two-component materials, resulting in asymmetric architectures in the 3- and 4-armed stars. This, of course, is different from the Vergina stars which have an equal number of arms of both components. Perhaps it would be better to look at the scaling behavior of two different series: (1) a series of $A_nB_n$ materials and (2) a series of $A_nB$ materials, both with increasing $n$. Neither the data nor the materials are currently available to do such a detailed study.

A prediction for the scaling behavior can be obtained by minimizing a simple Alexander−de Gennes scaling free energy per molecule with $n_1$ arms of block 1 and $n_2$ arms of block 2. This yields the following expression:

$$\frac{A}{R_g^2} = \frac{1}{R_g^2}\left(\frac{2}{\gamma}\right)^{1/3}\left\{n_1^3\left(\frac{V_1}{R_1}\right)^2 + n_2^3\left(\frac{V_2}{R_2}\right)^2\right\}^{1/3} \quad (1)$$

where $V_i$ is the volume of an arm of material $i$, $R_i$ is the unperturbed root-mean-square end-to-end distance of a single arm of material $i$, $\gamma$ is the interfacial energy per unit area, and $R_g$ is the radius of gyration of the entire star-shaped molecule. If we confine ourselves to systems such as the Vergina stars, which are symmetric with respect to arm number, the expression becomes

$$\frac{A}{R_g^2} = \frac{f}{2}\frac{1}{R_g^2}\left(\frac{2}{\gamma}\right)^{1/3}\left\{\left(\frac{V_1}{R_1}\right)^2 + \left(\frac{V_2}{R_2}\right)^2\right\}^{1/3} \quad (2)$$

from which it is evident $AN^{2/3}/R_g^2$ is expected to scale as $f^{1.0}$. This predicted behavior certainly falls within the range of experimentally determined scaling as delimited by the two curve fits in Figure 4. Physically we get an increasing spacing between molecules at the interface with increasing graft functionality. This results in more spreading of at least some of the arm trajectories parallel to the interface in molecules like the Vergina stars, which have high numbers of arms, relative to what one gets with linear diblocks.

## Conclusions

The three Vergina star samples investigated in this study all formed lamellar morphologies. For VS1 and VS2 with PS volume fractions of 0.44 and 0.47, respectively, the lamellar morphology was expected based on the theoretically predicted similarity of symmetric multiarm block copolymer behavior to that of simple diblocks. VS3, with a PS volume fraction of 0.37, is still in the region where diblocks would form lamella, but it is getting close to the transition to a cubic bicontinuous or cylindrical structure. We investigated the scaling of dimensionless, degree of polymerization corrected, interfacial area per molecule as a function of graft functionality across a series of diblocks, 3-armed miktoarm stars, 4-armed miktoarm stars, and Vergina stars. We find that $AN^{2/3}/R_g^2$ scales roughly as the first power of the graft point functionality. This reflects an increased spacing between the molecules at the interface and more spreading of at least some of the arm trajectories parallel to the interface.

**Acknowledgment.** S.P.G. acknowledges funding from the U.S. Army Research Office through Army Young Investigator Award DAAH04-95-1-0305. N.H. acknowledges the Greek General Secretariat of Research and Technology for financial support. We acknowledge the use of TEM instrumentation in the W. M. Keck Polymer Morphology Laboratory at the University of Massachusetts, Amherst, ARO instrumentation funding (DAAH04-95-1-0005), and Central Facility Support from the Materials Research Science and Engineering Center (MRSEC) at the University of Massachusetts, Amherst. We gratefully acknowledge Drs. Nora Beck Tan and Samuel F. Trevino of the Army Research Laboratory and NIST for access and help with small-angle neutron scattering. Darrin Pochan and Chin Lee also helped with the neutron scattering experiments.

## References and Notes

(1) Gido, S. P.; Lee, C.; Pochan, D. J.; Pispas, S.; Mays, J. W.; Hadjichristidis, N. *Macromolecules* **1996**, *29*, 7022.

(2) Pochan, D. J.; Gido, S. P.; Pispas, S.; Mays, J. W.; Ryan, A. J.; Fairclough, J. P. A.; Hamley, I. W.; Terrill, N. J. *Macromolecules* **1996**, *29*, 5091.

(3) Pochan, D. J.; Gido, S. P.; Pispas, S.; Mays, J. W. *Macromolecules* **1996**, *29*, 5099.

(4) Olvera de la Cruz, M.; Sanchez, I. C. *Macromolecules* **1986**, *19*, 2501.

(5) Milner, S. T. *Macromolecules* **1994**, *27*, 2333.

(6) Avgeropoulos, A.; Poulos, Y.; Hadjichristidis, N.; Roovers, J. *Macromolecules* **1996**, *29*, 6076.

(7) Hashimoto, T.; Shibayama, M.; Kawai, H. *Macromolecules* **1980**, *13*, 1237.

(8) Tselikas, Y.; Iatrou, H.; Hadjichristidis, N.; Liang, K. S.; Mohanty, K.; Lohse, D. J. *J. Chem. Phys.* **1996**, *105*, 2456.

(9) Yamakawa, H. *Modern Theory of Polymer Solutions*; Harper & Row: New York, 1971.

(10) Mays, J. W.; Hadjichristidis, N. *J. Appl. Polym. Sci., Appl. Polym. Symp.* **1992**, *51*, 55.

(11) Hadjichristidis, N. To be published.

(12) Daoud, M.; Cotton, J. P. *J. Phys.* **1982**, *43*, 531.

MA961855S